

Relic neutrino clustering and implications for their detection*

Andreas Ringwald and Yvonne Y. Y. Wong

Deutsches Elektronen-Synchrotron DESY, Hamburg, Germany
 andreas.ringwald@desy.de, yvonne.wong@desy.de

Summary. We study the gravitational clustering of big bang relic neutrinos onto existing cold dark matter and baryonic structures within the flat Λ CDM model. We then discuss the implications of clustering for scattering-based relic neutrino detection methods, ranging from flux detection via Cavendish-type torsion balances, to target detection using accelerator beams and cosmic rays.

1 Introduction

The standard big bang theory predicts the existence of 10^{87} neutrinos per flavour in the visible universe. This is an enormous abundance unrivalled by any other known form of matter, falling second only to the cosmic microwave background (CMB) photon. Yet, unlike the CMB which boasts its first detection in the 1960s and which has since been observed and its properties measured to high accuracy in a series of experiments, the relic neutrino continues to be elusive in the laboratory. The chief reason for this is of course the feebleness of the weak interaction. The smallness of the neutrino mass also makes momentum-transfer-based detection methods highly impractical. At present, the only evidence for the relic neutrino comes from inferences from other cosmological measurements, such as big bang nucleosynthesis, CMB and large scale structure (LSS) data (e.g., [2]). Nevertheless, it is difficult to accept that these neutrinos will never be detected in a more direct way.

In order to design feasible direct, scattering-based detection methods, a precise knowledge of the relic neutrino phase space distribution is indispensable. In this connection, it is important note that an oscillation interpretation of the atmospheric and solar neutrino data (e.g., [3]) implies that at least two of the neutrino mass eigenstates are nonrelativistic today. These neutrinos are subject to gravitational clustering on existing cold dark matter (CDM) and baryonic structures, possibly causing the local neutrino number density to depart from the standard value of $\bar{n}_\nu = \bar{n}_{\bar{\nu}} \simeq 56 \text{ cm}^{-3}$, and the momentum distribution to deviate from the relativistic Fermi-Dirac function.

In this talk, we describe a method that allows us to study the gravitational clustering of relic neutrinos onto CDM/baryonic structures. We calculate the present day neutrino overdensities in general CDM halos and in the Milky

* Talk given by YYW at DARK2004, College Station TX, USA. Based on [1].

Way, and then discuss their implications for scattering-based relic neutrino detection methods—from flux detection via Cavendish-type torsion balances, to target detection using accelerator beams and cosmic rays.

2 Vlasov equation

The standard procedure for any clustering investigation involving gravity only is to solve the Vlasov, or collisionless Boltzmann, equation (e.g., [4, 5]),

$$\frac{Df_i}{D\tau} \equiv \frac{\partial f_i}{\partial \tau} + \dot{\mathbf{x}} \cdot \frac{\partial f_i}{\partial \mathbf{x}} + \dot{\mathbf{p}} \cdot \frac{\partial f_i}{\partial \mathbf{p}} = 0. \quad (1)$$

The single-particle phase density $f_i(\mathbf{x}, \mathbf{p}, \tau)$ is defined so that $dN_i = f_i d^3x d^3p$ is the number of i type particles (e.g., CDM, neutrinos) in an infinitesimal phase space volume element. The variables $\mathbf{x} = \mathbf{r}/a(t)$, $\mathbf{p} = am_i\dot{\mathbf{x}}$, and $d\tau = dt/a(t)$ are the comoving distance, its associated conjugate momentum, and the conformal time respectively, with a as the scale factor and m_i the mass of the i th particle species. All temporal and spatial derivatives are taken with respect to comoving coordinates, i.e., $\cdot \equiv \partial/\partial\tau$, $\nabla \equiv \partial/\partial\mathbf{x}$.²

In the nonrelativistic, Newtonian limit, equation (1) is equivalent to

$$\frac{\partial f_i}{\partial \tau} + \frac{\mathbf{p}}{am_i} \cdot \frac{\partial f_i}{\partial \mathbf{x}} - am_i \nabla \phi \cdot \frac{\partial f_i}{\partial \mathbf{p}} = 0, \quad (2)$$

with the Poisson equation

$$\nabla^2 \phi = 4\pi G a^2 \sum_i \bar{\rho}_i(\tau) \delta_i(\mathbf{x}, \tau), \quad (3)$$

$$\delta_i(\mathbf{x}, \tau) \equiv \frac{\rho_i(\mathbf{x}, \tau)}{\bar{\rho}_i(\tau)} - 1, \quad \rho_i(\mathbf{x}, \tau) = \frac{m_i}{a^3} \int d^3p f_i(\mathbf{x}, \mathbf{p}, \tau), \quad (4)$$

relating the peculiar gravitational potential $\phi(\mathbf{x}, \tau)$ to the density fluctuations $\delta_i(\mathbf{x}, \tau)$ with respect to the physical mean $\bar{\rho}_i(\tau)$.

The Vlasov equation expresses conservation of phase space density f_i along each characteristic $\{\mathbf{x}(\tau), \mathbf{p}(\tau)\}$ given by

$$\frac{d\mathbf{x}}{d\tau} = \frac{\mathbf{p}}{am_i}, \quad \frac{d\mathbf{p}}{d\tau} = -am_i \nabla \phi. \quad (5)$$

The complete set of characteristics coming through every point in phase space is thus exactly equivalent to equation (1). It is generally not possible to follow the whole set of characteristics, but the evolution of the system can still be traced, to some extent, if we follow a sufficiently large but still manageable sample selected from the initial phase space distribution. This forms the basis of particle-based solution methods.

² Unless otherwise indicated, comoving spatial and temporal quantities are used throughout the present work. Masses and densities, however, are always physical.

3 Solution method and halo density profiles

A “first principles” approach to neutrino clustering requires the simultaneous solution of the Vlasov equation (1) for both CDM and neutrinos. This is usually done by means of multi-component N -body simulations. In our treatment, however, we make two simplifying approximations:

1. We assume only the CDM component ρ_m contributes to ϕ in the Poisson equation (3), and ρ_m to be completely specified by halo density profiles from high resolution Λ CDM simulations [6]. The neutrino component is treated as a small perturbation whose clustering depends on the CDM halo profile, but is too small to affect it in return. This assumption is well justified, since, on cosmological scales, LSS data require $\rho_\nu/\rho_m = \Omega_\nu/\Omega_m < 0.2$ [2]. On cluster/galactic scales, neutrino free-streaming ensures that ρ_ν/ρ_m always remains smaller than Ω_ν/Ω_m [7].
2. Given that assumption 1. holds, it follows that not only will the CDM halo be gravitationally blind to the neutrinos, the neutrinos themselves will also have negligible gravitational interaction with each other.

These approximations together allow us to track the neutrinos one at a time in N independent simulations, instead of following N particles simultaneously in one single run. We shall call this “ N -one-body simulation” [1].

For the halo density profiles, we use the “universal profile” advocated by Navarro, Frenk and White (hereafter, NFW) [8, 9],

$$\rho_{\text{halo}}(r) = \frac{\rho_s}{(r/r_s)(1+r/r_s)^2}. \quad (6)$$

The parameters r_s and ρ_s are determined by the halo’s virial mass M_{vir} and a dimensionless concentration parameter $c \equiv r_{\text{vir}}/r_s$, where r_{vir} is the virial radius, within which lies M_{vir} of matter with an average density equal to δ_{TH} times the mean matter density $\bar{\rho}_m$ at that redshift, i.e.,

$$M_{\text{vir}} \equiv \frac{4\pi}{3} \delta_{\text{TH}} \bar{\rho}_m a^3 r_{\text{vir}}^3 = \frac{4\pi}{3} \delta_{\text{TH}} \bar{\rho}_{m,0} r_{\text{vir}}^3, \quad (7)$$

where $\bar{\rho}_{m,0}$ is the present day mean matter density. The factor δ_{TH} is the overdensity predicted by the dissipationless spherical top-hat collapse model,

$$\delta_{\text{TH}} \simeq \frac{18\pi^2 + 82y - 39y^2}{\Omega_m(z)}, \quad y = \Omega_m(z) - 1, \quad (8)$$

with $\Omega_m(z) = \Omega_{m,0}/(\Omega_{m,0} + \Omega_{\Lambda,0}a^3)$ [10].

Furthermore, halo concentration correlates with its mass. At $z = 0$, the trend

$$c(z = 0) \simeq 9 \left(\frac{M_{\text{vir}}}{1.5 \times 10^{13} h^{-1} M_\odot} \right)^{-0.13} \quad (9)$$

was found in [11]. In addition, for a fixed virial mass, the median concentration parameter exhibits a redshift dependence of $c(z) \simeq c(z = 0)/(1 + z)$ between $z = 0$ and $z = 4$.

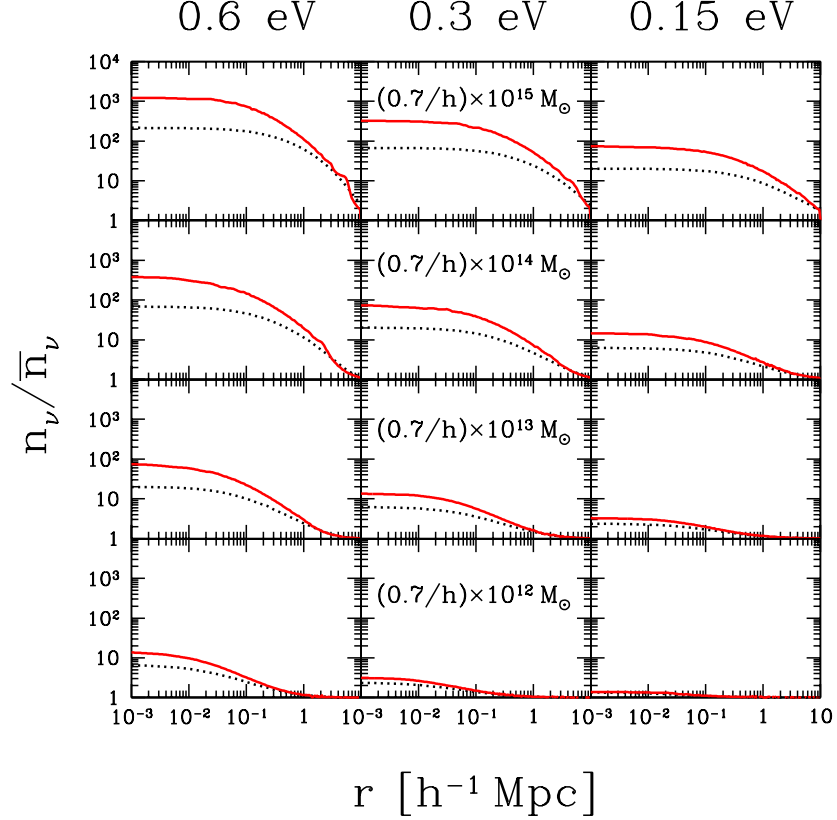


Fig. 1. Relic neutrino number density per flavour, $n_\nu = n_{\bar{\nu}}$, normalised to $\bar{n}_\nu = \bar{n}_{\bar{\nu}} \simeq 56 \text{ cm}^{-3}$, for the indicated neutrino and halo virial masses. Results from N -one-body simulations are denoted by red (solid) lines. Dotted lines correspond to overdensities calculated with the linear approximation.

4 Clustering in NFW halos

Using the NFW halo profile (6) as an input, we find solutions to the Vlasov equation in the limit $\rho_\nu \ll \rho_m$. The CDM distribution is modelled as follows: We assume a uniform distribution of CDM throughout space, with a spherical NFW halo sitting at the origin. For the neutrinos, we take their initial distribution to be the homogeneous and isotropic Fermi-Dirac distribution with no chemical potential. The initial redshift is taken to be $z = 3$, since, at higher redshifts, a sub-eV neutrino has too much thermal velocity to cluster efficiently. The cosmological parameters used are $\{\Omega_m, \Omega_\Lambda, h\} = \{0.3, 0.7, 0.7\}$.

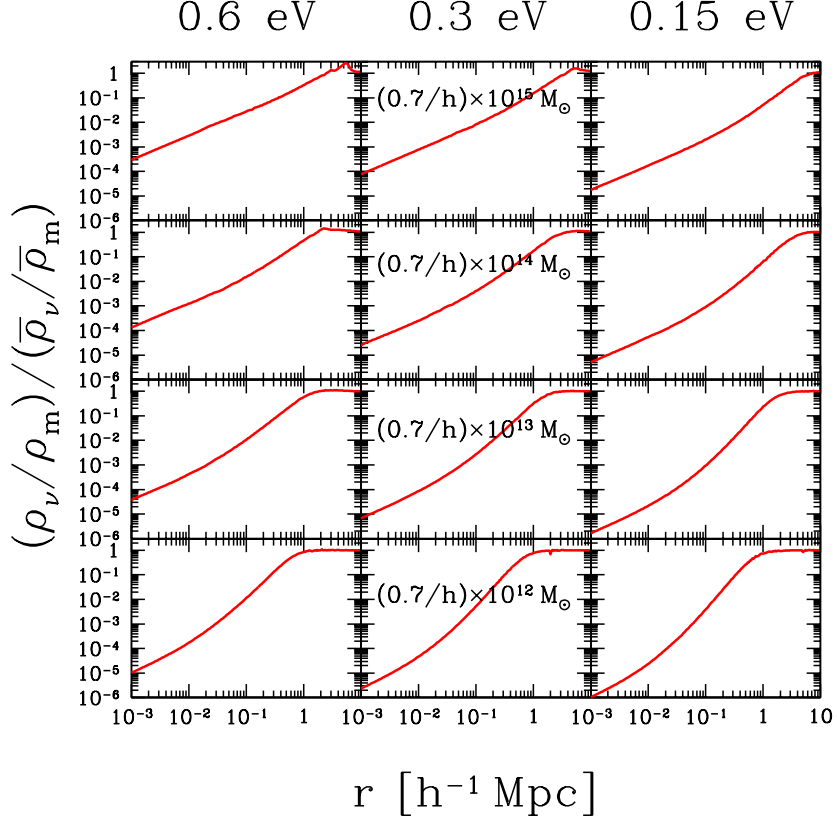


Fig. 2. Mass density ratio ρ_ν/ρ_m normalised to the background mean $\bar{\rho}_\nu/\bar{\rho}_m$ obtained from N -one-body simulations for the indicated neutrino and halo masses.

We solve the Vlasov equation using N -one-body simulations, as well as a semi-analytical linear method.³ The essential features of the results (Figures 1 and 2) can be understood in terms of neutrino free-streaming, which causes n_ν/\bar{n}_ν to flatten out at small radii, and the mass density ratio ρ_ν/ρ_m to drop substantially below the background mean. Both n_ν/\bar{n}_ν and ρ_ν/ρ_m approach their respective cosmic mean of 1 and $\bar{\rho}_\nu/\bar{\rho}_m$ at large radii.

Furthermore, we find that the linear method systematically underestimates the neutrino overdensities over the whole range of halo and neutrino masses considered here. Reconciliation with N -one-body simulations can only be achieved if we impose a smoothing scale of > 1 Mpc, or if $n_\nu/\bar{n}_\nu < 3 \div 4$.

³ The linear approximation [12] consists of replacing $\partial f/\partial \mathbf{p}$ with $\partial f_0/\partial \mathbf{p}$ in (1), where f_0 is the unperturbed Fermi-Dirac function.

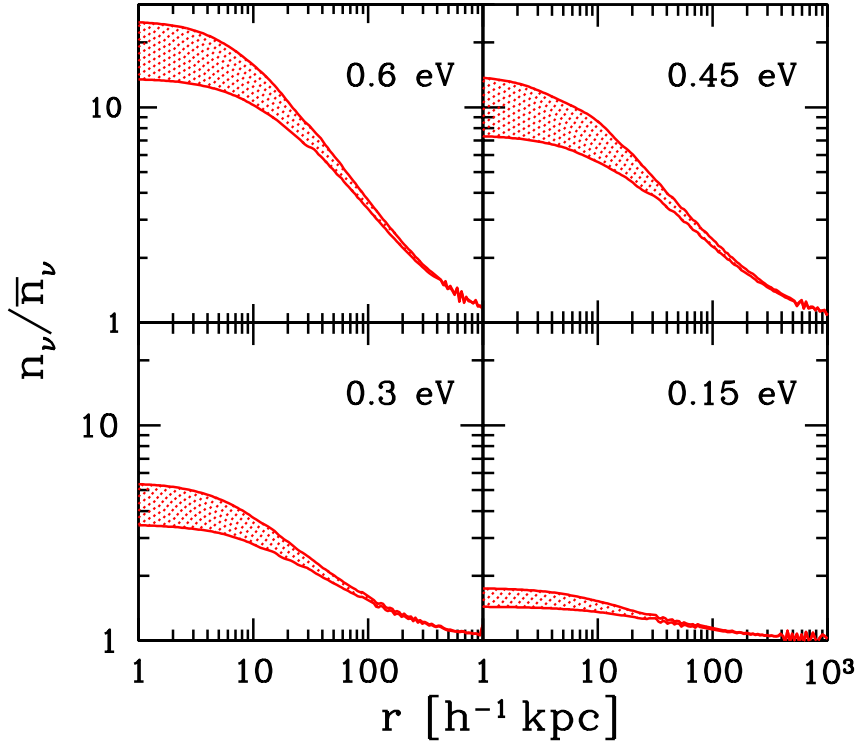


Fig. 3. Relic neutrino number density per flavour, $n_\nu = n_{\bar{\nu}}$, in the Milky Way for various neutrino masses. All curves are normalised to $\bar{n}_\nu = \bar{n}_{\bar{\nu}} \simeq 56 \text{ cm}^{-3}$. The top curve in each plot corresponds to the MWnow run, and the bottom to the NFWhalo run. The enclosed region represents a possible range of overdensities at $z = 0$.

This finding is consistent with the standard lore that perturbative methods fail once the perturbations exceed unity and nonlinear effects set in.

5 Clustering in the Milky Way

In order to calculate the neutrino overdensity in the Milky Way and, especially, their phase space distribution at Earth ($r_\oplus \sim 8 \text{ kpc}$ from the Galactic Centre), we need, in principle, to know the complete assembly history of the Milky Way. Theory suggests that the galactic bulge and disk grew out of an NFW halo via baryonic compression [13, 14]. Our strategy, then, is to conduct two series of simulations, one for the present day Milky Way mass

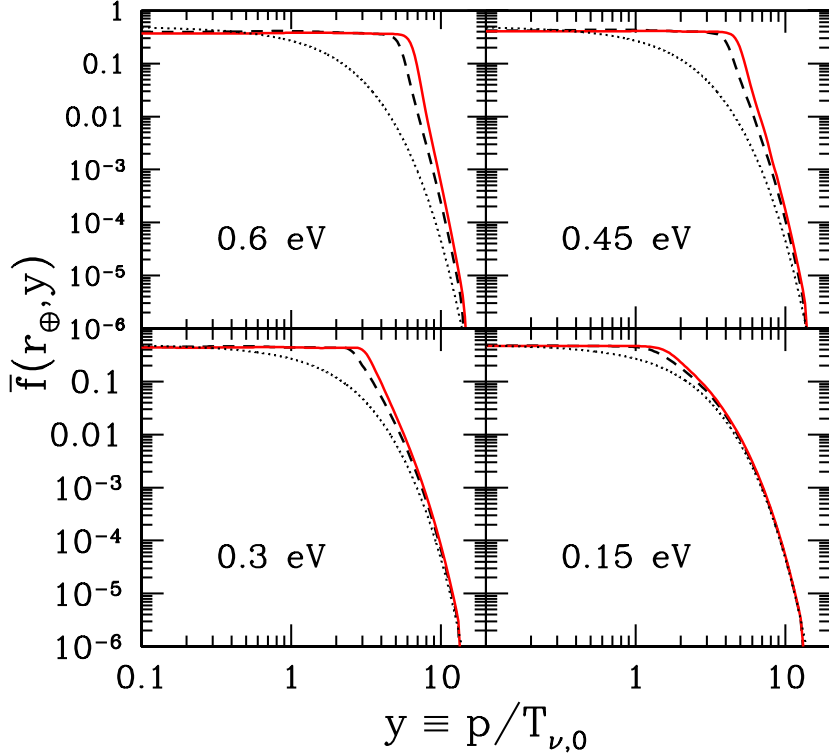


Fig. 4. Momentum distribution of relic neutrinos at r_{\oplus} for various neutrino masses. The red (solid) line denotes the MWnow run, while the dashed line represents the NFWhalo run. The relativistic Fermi-Dirac function is indicated by the dotted line. The escape velocity $v_{\text{esc}} = \sqrt{2|\phi(r_{\oplus})|}$ is 490 km s $^{-1}$ and 450 km s $^{-1}$ for MWnow and NFWhalo respectively, corresponding to “escape momenta” $y_{\text{esc}} \equiv m_{\nu} v_{\text{esc}} / T_{\nu,0}$ of (5.9, 4.4, 3.0, 1.5) and (5.4, 4.1, 2.7, 1.4) for $m_{\nu} = (0.6, 0.45, 0.3, 0.15)$ eV.

distribution (MWnow) [15, 16] which we assume to be static, and one for the NFW halo (NFWhalo) that would have been there, had baryon compression not taken place. The real neutrino overdensity should then lie somewhere between these two extremes. Figure 3 shows the possible ranges of overdensities at $z = 0$.

In all cases, the final momentum distribution at r_{\oplus} is almost isotropic, with a zero mean radial velocity $\langle v_r \rangle$, and second velocity moments that satisfy approximately the relation $2\langle v_r^2 \rangle = \langle v_T^2 \rangle$. Hence, we plot the coarse-

grained phase space densities $\bar{f}(r_{\oplus}, p)$ only as functions of the absolute velocity.

The coarse-grained spectra in Figure 4 show varying degrees of deviation from the relativistic Fermi–Dirac function, but share a common feature that $\bar{f} \sim 1/2$ up to the momentum state corresponding to the escape velocity from the Milky Way at r_{\oplus} . This agrees with the requirement that the final coarse-grained density must not exceed the maximal initial fine-grained distribution, $\bar{f} \leq \max(f_0)$ [17, 18, 19, 20, 21]. For neutrinos, $\max(f_0) = 1/2$ at $p = 0$. Thus, our \bar{f} not only satisfies but completely saturates the bound up to p_{esc} , forming a semi-degenerate state that can only be made denser by filling in states above p_{esc} .⁴

6 Relic neutrino detection

6.1 Flux detection

The relic neutrinos’ low average momentum $\langle p \rangle = \langle y \rangle T_{\nu,0}$ corresponds to a de Broglie wavelength of macroscopic dimension, $\lambda = 1/\langle p \rangle = 0.12 \text{ cm}/\langle y \rangle$. Therefore, one may envisage scattering processes in which many target atoms act coherently [22, 23] over a macroscopic volume λ^3 , so that the elastic scattering rate is proportional to the square of the number of target atoms in λ^3 . Compared to the case where the neutrinos are elastically scattered coherently only on the individual target nuclei, the new rate is enhanced by a factor of

$$\frac{N_A}{A} \rho_t \lambda^3 \simeq 6 \times 10^{18} \left(\frac{100}{A} \right) \left(\frac{\rho_t}{\text{g/cm}^3} \right) \left(\frac{\lambda}{0.1 \text{ cm}} \right)^3, \quad (10)$$

where N_A is the Avogadro constant, A is the atomic mass, and ρ_t is the mass density of the target material.⁵

Exploiting this effect, a practical detection scheme for the local relic neutrino flux is based on the fact that a test body of density ρ_t at Earth experiences a neutrino wind force through random scattering events, leading to an acceleration given, for Dirac neutrinos, by [22, 23, 27, 28]

$$\begin{aligned} a_t &\simeq \sum_{\nu, \bar{\nu}} \underbrace{n_{\nu} v_{\text{rel}}}_{\text{flux}} \frac{4\pi}{3} N_A^2 \rho_t r_t^3 \underbrace{\sigma_{\nu N}}_{\text{mom. transfer}} \underbrace{2 m_{\nu} v_{\text{rel}}}_{\text{}} \\ &\simeq 2 \times 10^{-28} \left(\frac{n_{\nu}}{\bar{n}_{\nu}} \right) \left(\frac{10^{-3} c}{v_{\text{rel}}} \right) \left(\frac{\rho_t}{\text{g/cm}^3} \right) \left(\frac{r_t}{\hbar/(m_{\nu} v_{\text{rel}})} \right)^3 \text{ cm s}^{-2}, \end{aligned} \quad (11)$$

⁴ This degeneracy should not be confused with that arising from the Pauli exclusion principle.

⁵ In the case of coherent scattering, it is possible, in principle, to measure also the scattering amplitude itself [24, 25, 26], which is linear in G_F . However, a large lepton asymmetry is required for a non-negligible effect.

with $r_t < \lambda$, $\sigma_{\nu N} \simeq G_F^2 m_\nu^2 / \pi$ is the elastic neutrino–nucleon cross section, $v_{\text{rel}} = \langle |\mathbf{v} - \mathbf{v}_\oplus| \rangle$ the mean neutrino velocity in the detector’s rest frame, and $v_\oplus \simeq 2.3 \times 10^2 \text{ km s}^{-1} \simeq 7.7 \times 10^{-4} c$ the Earth’s velocity through the Milky Way. For $n_\nu / \bar{n}_\nu \sim 20$, equation (11) gives $a_t \sim 10^{-26} \text{ cm s}^{-2}$. For Majorana neutrinos, a_t is further suppressed by a factor of $(v_{\text{rel}}/c)^2 \simeq 10^{-6}$ for an unpolarised target, and $v_{\text{rel}}/c \simeq 10^{-3}$ for a polarised one.

To digest these estimates, we note that the smallest measurable acceleration at present is $> 10^{-13} \text{ cm s}^{-2}$, using conventional Cavendish-type torsion balances. Possible improvements with currently available technology to a sensitivity of $> 10^{-23} \text{ cm s}^{-2}$ have been proposed [29, 30]. However, this is still off the prediction (11) by three orders of magnitude. Therefore, we conclude that an observation of this effect will not be possible in the next decade, but can still be envisaged in the foreseeable future (thirty to forty years according to [32], exploiting advances in nanotechnology), if our known light neutrinos are Dirac particles. Should they turn out, in the meantime, to be Majorana particles, flux detection via mechanical forces will be a real challenge.

Lastly, the background contribution to the acceleration (11) from the solar pp neutrinos [flux $\sim 10^{11} \text{ cm}^{-2} \text{s}^{-1}$, $\langle E_\nu \rangle \sim 0.3 \text{ MeV}$ (e.g., [31])], $a_t^{\nu \text{ sun}} \simeq 10^{-27} \text{ cm s}^{-2}$ [27], may be rejected by directionality. The background from weakly interacting massive particles (WIMPs χ , with mass m_χ) [27],

$$a_t^{\text{WIMP}} \simeq \underbrace{n_\chi v_{\text{rel}}}_{\text{flux}} \underbrace{N_A A \sigma_{\chi N}}_{\text{mom. transfer}} \underbrace{2 m_\chi v_{\text{rel}}}_{\text{}} \quad (12)$$

$$\simeq 6 \times 10^{-29} \left(\frac{\rho_\chi}{0.3 \text{ GeV/cm}^3} \right) \left(\frac{v_{\text{rel}}}{10^{-3} c} \right)^2 \left(\frac{A}{100} \right) \left(\frac{\sigma_{\chi N}}{10^{-45} \text{ cm}^2} \right) \text{ cm s}^{-2},$$

should they be the main constituent of galactic dark matter with mass density $\rho_\chi \equiv n_\chi m_\chi \simeq 0.3 \text{ GeV cm}^{-3}$ at r_\oplus , can be neglected as soon as the WIMP–nucleon cross section $\sigma_{\chi N}$ is smaller than $\sim 3 \times 10^{-45} \text{ cm}^2$. This should be well established by the time relic neutrino direct detection becomes a reality.

6.2 Target detection

Detection methods based on the scattering of extremely energetic particles (accelerator beams or cosmic rays) off the relic neutrinos as a target take advantage of the fact that, for centre-of-mass (c.m.) energies,

$$\sqrt{s} = \sqrt{2 m_\nu E_{\text{beam}}} \simeq 4.5 \left(\frac{m_\nu}{\text{eV}} \right)^{1/2} \left(\frac{E_{\text{beam}}}{10 \text{ TeV}} \right)^{1/2} \text{ MeV}, \quad (13)$$

just below the W - and Z -resonances, the weak interaction cross sections grow rapidly with the beam energy E_{beam} .

At accelerators Target detection using accelerator beams does not seem viable. For a hypothetical beam energy of 10^7 TeV and an accelerator ring of ultimate circumference $L \simeq 4 \times 10^4 \text{ km}$ around the Earth, the interaction rate is roughly one event per year. See [1] for details.

With cosmic rays It was pointed out by Weiler [33, 34] (for earlier suggestions, see [35, 36, 37, 38, 39]) that the resonant annihilation of extremely energetic cosmic neutrinos (EEC ν)—with $E > 10^{20}$ eV—with relic anti-neutrinos (and vice versa) into Z -bosons appears to be a unique process having sensitivity to the relic neutrinos. On resonance,

$$E_\nu^{\text{res}} = \frac{m_Z^2}{2m_\nu} \simeq 4 \times 10^{21} \left(\frac{\text{eV}}{m_\nu} \right) \text{ eV}, \quad (14)$$

the associated cross section is enhanced by several orders of magnitude,

$$\langle \sigma_{\text{ann}} \rangle = \int ds \sigma_{\nu\bar{\nu}}^Z(s)/m_Z^2 \simeq 2\pi\sqrt{2} G_F \simeq 4 \times 10^{-32} \text{ cm}^2, \quad (15)$$

leading to a “short” mean free path $\ell_\nu = (\bar{n}_\nu \langle \sigma_{\text{ann}} \rangle)^{-1} \simeq 1.4 \times 10^5$ Mpc which is *only* about $48h$ times the Hubble distance. Neglecting cosmic evolution effects, this corresponds to an annihilation probability for EEC ν from cosmological distances on the relic neutrinos of $2h^{-1}\%$.

The signatures of annihilation are (i) absorption dips [33, 34, 40] (see also [41, 42, 43]) in the EEC ν spectrum at the resonant energies, and (ii) emission features [44, 45, 46, 47, 48] (Z -bursts) as protons and photons with energies spanning a decade or more above the Greisen–Zatsepin–Kuzmin (GZK) cutoff at $E_{\text{GZK}} \simeq 4 \times 10^{19}$ eV [49, 50]. This is the energy beyond which the CMB is absorbing to nucleons due to resonant photopion production.⁶

The possibility to confirm the existence of relic neutrinos within the next decade from a measurement of the aforementioned dips in the EEC ν flux was recently investigated in [40]. Presently planned neutrino detectors (Pierre Auger Observatory [55], IceCube [56], ANITA [57], EUSO [58], OWL [59], and Salsa [60]) operating in the energy regime above 10^{21} eV appear to be sensitive enough to lead us, within the next decade, into an era of relic neutrino absorption spectroscopy, provided that the EEC ν flux at the resonant energies is close to current observational bounds and the neutrino mass is > 0.1 eV. In this case, the associated Z -bursts must also be seen as post-GZK events at the planned cosmic ray detectors (Auger, EUSO, and OWL).

What are the implications of relic neutrino clustering for absorption and emission spectroscopy? Firstly, absorption spectroscopy is predominantly sensitive to the relic neutrino background at early times, with the depths of the absorption dips determined largely by the higher number densities at $z \gg 1$. Since neutrinos do not cluster significantly until $z < 2$, clustering at recent times can only show up as secondary dips with such minimal widths in energy [61] that they do not seem likely to be resolved by planned observatories.

On the other hand, emission spectroscopy is directly sensitive to the relic neutrino content of the local universe ($z < 0.01 \Leftrightarrow r_{\text{GZK}} < 50$ Mpc). However,

⁶ The association of Z -bursts with the mysterious cosmic rays observed above E_{GZK} is a controversial possibility [44, 45, 46, 47, 48, 51, 52, 53, 54].

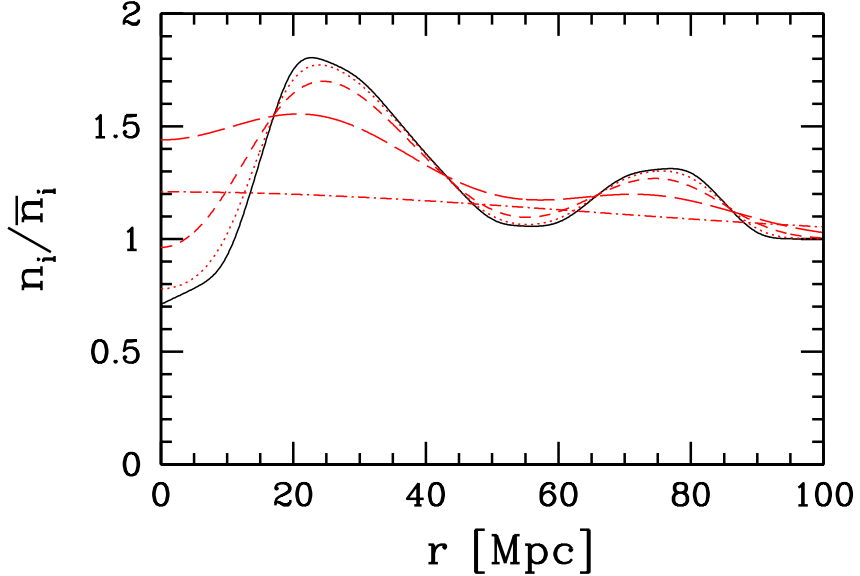


Fig. 5. “Large scale” overdensities ($i = \nu, \text{CDM}$) in the local universe, with the Milky Way at $r = 0$. The black (solid) line corresponds to the local CDM distribution inferred from peculiar velocity measurements [62] (see also [63]) smeared over the surface of a sphere with radius r [48]. The dotted line is the neutrino overdensity for $m_\nu = 0.6$ eV, short dash 0.3 eV, long dash 0.15 eV, and dot-dash 0.04 eV.

since the neutrino density contrasts approximately track those of the underlying CDM above the neutrino free-streaming scale k_{fs}^{-1} , it is clear that there cannot be a substantial neutrino overdensity over the whole GZK volume ($\sim r_{\text{GZK}}^3$). Indeed, given the local CDM distribution inferred from peculiar velocity measurements (smeared over ~ 5 Mpc), we estimate the corresponding neutrino overdensity to be < 2 (Figure 5). Hence the overall emission rate cannot be significantly enhanced by gravitational clustering.

Another possibility is to exploit the fact that there are several galaxy clusters ($> 10^{14} M_\odot$) within the GZK zone with significant neutrino clustering. One could then search for directional dependences in the emission events as a signature of EEC ν –relic ν annihilation. For example, AGASA has an angular resolution of $\sim 2^\circ$ [64]. This is already sufficient to resolve the internal structures of, say, the Virgo cluster (distance ~ 15 Mpc, $M_{\text{vir}} \sim 8 \times 10^{14} M_\odot$) which spans some 10° across the sky. From Figure 1, the average neutrino overdensity along the line of sight towards and up to Virgo is estimated to be ~ 45 and ~ 5 for $m_\nu = 0.6$ eV and 0.15 eV respectively, given an angular resolution of $\sim 2^\circ$. The corresponding increases in the number of events coming from the direction of the Virgo cluster relative to the unclustered

case, assuming an isotropic distribution of $\text{EEC}\nu$ sources, are given roughly by the same numbers, since protons originating from ~ 15 Mpc away arrive at Earth approximately unattenuated. The numbers improve to ~ 55 and ~ 8 respectively with a finer $\sim 1^\circ$ angular resolution.

7 Conclusion

We have conducted a systematic and exhaustive study of the gravitational clustering of big bang relic neutrinos onto existing CDM and baryonic structures within the flat Λ CDM model. Our main computational tools are (i) a restricted, N -one-body method, in which we neglect the gravitational interaction between the neutrinos and treat them as test particles moving in an external potential generated by the CDM/baryonic structures, and (ii) a semi-analytical, linear technique, which requires additional assumptions about the neutrino phase space distribution. In both cases, the CDM/baryonic gravitational potentials are calculated from parametric halo density profiles from high resolution N -body studies and/or from realistic mass distributions reconstructed from observational data.

Using these two techniques, we track the relic neutrinos' accretion onto CDM halos ranging from the galaxy to the galaxy cluster variety ($M_{\text{vir}} \sim 10^{12} \rightarrow 10^{15} M_\odot$), and determine the neutrino number densities on scales $\sim 1 \rightarrow 1000$ kpc for a range of neutrino masses. We find that the linear method systematically underestimates the neutrino overdensities over the whole range of halo and neutrino masses considered. Reconciliation with N -one-body simulations can only be achieved if we impose a smoothing scale of > 1 Mpc, or if the overdensity is no more than three or four. We therefore conclude that the linear theory does not generally constitute a faithful approximation to the Vlasov equation in the study of neutrino clustering on galactic and sub-galactic scales (< 50 kpc). However, it may still be useful for finding the minimum effects of neutrino clustering in other contexts not considered in this work (e.g., the nonlinear matter power spectrum [65]).

Next we estimate the neutrino phase space distribution in the Milk Way, especially in our local neighbourhood at Earth r_\oplus , taking also into account contributions to the total gravitational potential from the galactic bulge and disk. We find a maximum overdensity of ~ 20 per neutrino flavour in our immediate vicinity, provided that the neutrino mass is at its current upper limit of 0.6 eV. For neutrino masses less than 0.15 eV, the expected overdensity from gravitational clustering is less than two. The associated coarse-grained momentum spectra show varying degrees of deviation from the relativistic Fermi-Dirac function, but share a common feature that they are semi-degenerate, with phase space density $\bar{f} \sim 1/2$, up to the momentum state corresponding to the escape velocity from the Milky Way at r_\oplus . This means that the neutrino number densities we have calculated here for r_\oplus are already the *highest possible*, given the neutrino mass, without violating

phase space constraints. In order to attain even higher densities, one must now appeal to non-standard theories (e.g., [66]).

In terms of scattering-based detection possibilities, this meager enhancement in the neutrino number density in the Milky Way from gravitational clustering means that relic neutrinos are still far from being detected in fully earthbound laboratory experiments. For flux detection methods based on coherent elastic scattering of relic neutrinos off target matter in a terrestrial detector, a positive detection could be thirty to forty years away, provided that light neutrinos are Dirac particles. For light Majorana neutrinos, another $\sim 10^3$ times more sensitivity would be required in the detector for a positive signal. Target detection methods using accelerator beams seem equally hopeless, unless the accelerator is the size of the Earth and operates at an energy of $\sim 10^7$ TeV.

Meanwhile, target detection using extremely energetic cosmic neutrinos ($\text{EEC}\nu, > 10^{21}$ eV) remains the only viable means to confirm the existence of big bang relic neutrinos within the next decade or so. Resonant annihilation of $\text{EEC}\nu$ on relic neutrinos can be revealed as absorption dips in the $\text{EEC}\nu$ flux (e.g., [40]), or as emission features in the Z -decay products. However, since absorption spectroscopy is largely insensitive to late time ($z < 2$) relic neutrino clustering, our findings here have little impact on the conclusions of [40]. On the other hand, emission spectroscopy is sensitive to the relic neutrino content of the local GZK zone, $V_{\text{GZK}} \sim 50^3$ Mpc³. While we find no significant large scale clustering within V_{GZK} and therefore no significant enhancement in the overall emission rates, it is still conceivable to exploit the considerable neutrino overdensities in nearby galaxy clusters, and search for directional dependences in the post-GZK emission events. For the Virgo cluster, for example, we estimate the event rate from the central 1° region to be ~ 55 and ~ 8 times the unclustered rate for neutrino mass $m_\nu = 0.6$ eV and 0.15 eV respectively, assuming an isotropic distribution of $\text{EEC}\nu$ sources. Planned observatories such as the Pierre Auger Observatory [55], EUSO [58] and OWL [59] will have sufficient angular resolution to, in principle, see this enhancement. However, considering the rapidly improving constraints on both the $\text{EEC}\nu$ flux and neutrino masses, it remains to be seen if the enhancement can indeed be observed with enough statistical significance [67].

References

1. A. Ringwald and Y. Y. Y. Wong, JCAP **0412** (2004) 005 [arXiv:hep-ph/0408241].
2. S. Hannestad, New J. Phys. 6 (2004) **108** [arXiv:hep-ph/0404239].
3. G. L. Fogli, E. Lisi, A. Marrone, D. Montanino, A. Palazzo and A. M. Rotunno, eConf **C030626** (2003) THAT05 [arXiv:hep-ph/0310012].
4. E. Bertschinger, in *Les Houches Cosmology 1993*, pp. 273-348, arXiv:astro-ph/9503125.

5. A. Klypin, in *Modern Cosmology*, edited by S. Bonometto, V. Gorini, and U. Moschella (IOP, Bristol, 2002), p. 420.
6. S. Singh and C. P. Ma, Phys. Rev. D **67** (2003) 023506 [arXiv:astro-ph/0208419].
7. L. Kofman, A. Klypin, D. Pogosian and J. P. Henry, Astrophys. J. **470** (1996) 102 [arXiv:astro-ph/9509145].
8. J. F. Navarro, C. S. Frenk and S. D. M. White, Astrophys. J. **462** (1996) 563 [arXiv:astro-ph/9508025].
9. J. F. Navarro, C. S. Frenk and S. D. M. White, Astrophys. J. **490** (1997) 493.
10. G. L. Bryan and M. L. Norman, Astrophys. J. **495** (1998) 80 [arXiv:astro-ph/9710107].
11. J. S. Bullock *et al.*, Mon. Not. Roy. Astron. Soc. **321** (2001) 559 [arXiv:astro-ph/9908159].
12. I. H. Gilbert, Astrophys. J. **144** (1966) 233.
13. S. D. M. White and M. J. Rees, Mon. Not. Roy. Astro. Soc. **183** (1978) 341.
14. H. J. Mo, S. Mao and S. D. M. White, Mon. Not. Roy. Astron. Soc. **295** (1998) 319 [arXiv:astro-ph/9707093].
15. W. Dehnen and J. Binney, Mon. Not. Roy. Astro. Soc. **294** (1998) 429 [arXiv:astro-ph/9612059].
16. A. Klypin, H. Zhao and R. S. Somerville, Astrophys. J. **573** (2002) 597 [arXiv:astro-ph/0110390].
17. D. Lynden-Bell, Mon. Not. Roy. Astron. Soc. **136** (1967) 101.
18. S. Tremaine and J. E. Gunn, Phys. Rev. Lett. **42** (1979) 407.
19. F. H. Shu, Astrophys. J. **225** (1978) 83.
20. F. H. Shu, Astrophys. J. **316** (1987) 502.
21. A. Kull, R. A. Treumann and H. Böhringer, Astrophys. J. **466** (1996) L1 [arXiv:astro-ph/9606057].
22. B. F. Shvartsman, V. B. Braginsky, S. S. Gershtein, Y. B. Zeldovich and M. Y. Khlopov, JETP Lett. **36** (1982) 277 [Pisma Zh. Eksp. Teor. Fiz. **36** (1982) 224].
23. P. F. Smith and J. D. Lewin, Phys. Lett. B **127** (1983) 185.
24. L. Stodolsky, Phys. Rev. Lett. **34** (1975) 110 [Erratum-ibid. **34** (1975) 508].
25. N. Cabibbo and L. Maiani, Phys. Lett. B **114** (1982) 115.
26. P. Langacker, J. P. Leveille and J. Sheiman, Phys. Rev. D **27** (1983) 1228.
27. G. Duda, G. Gelmini and S. Nussinov, Phys. Rev. D **64** (2001) 122001 [arXiv:hep-ph/0107027].
28. I. Ferreras and I. Wasserman, Phys. Rev. D **52** (1995) 5459.
29. C. Hagmann, in *COSMO98: Proceedings of the Conference on Particle Physics and the Early Universe*, edited by D. O. Caldwell (AIP, Woodbury NY, 1999), p.460 [AIP Conf. Proc. **478** (1998) 460; arXiv:astro-ph/9902102].
30. C. Hagmann, presented at *American Physical Society (APS) Meeting of the Division of Particles and Fields (DPF 99)*, Los Angeles, USA, 1999, arXiv:astro-ph/9905258.
31. J. N. Bahcall, M. H. Pinsonneault and S. Basu, Astrophys. J. **555** (2001) 990 [arXiv:astro-ph/0010346].
32. P. F. Smith, Phil. Trans. Roy. Soc. Lond. A **361** (2003) 2591.
33. T. J. Weiler, Phys. Rev. Lett. **49** (1982) 234.
34. T. J. Weiler, Astrophys. J. **285** (1984) 495.
35. J. Bernstein, M. Ruderman and G. Feinberg, Phys. Rev. **132** (1963) 1227.

36. B. P. Konstantinov and G. E. Kocharov, *J. Exp. Theor. Phys.* **19** (1964) 992.
37. R. Cowsik, Y. Pal and S. N. Tandon, *Phys. Lett.* **13** (1964) 265.
38. T. Hara and H. Sato, *Prog. Theor. Phys.* **64** (1980) 1089.
39. T. Hara and H. Sato, *Prog. Theor. Phys.* **65** (1981) 477.
40. B. Eberle, A. Ringwald, L. Song and T. J. Weiler, *Phys. Rev. D* **70** (2004) 023007 [arXiv:hep-ph/0401203].
41. P. Gondolo, G. Gelmini and S. Sarkar, *Nucl. Phys. B* **392** (1993) 111 [arXiv:hep-ph/9209236].
42. E. Roulet, *Phys. Rev. D* **47** (1993) 5247.
43. S. Yoshida, H. Y. Dai, C. C. Jui and P. Sommers, *Astrophys. J.* **479** (1997) 547 [arXiv:astro-ph/9608186].
44. D. Fargion, B. Mele and A. Salis, *Astrophys. J.* **517** (1999) 725 [arXiv:astro-ph/9710029].
45. T. J. Weiler, *Astropart. Phys.* **11** (1999) 303 [arXiv:hep-ph/9710431].
46. S. Yoshida, G. Sigl and S. J. Lee, *Phys. Rev. Lett.* **81** (1998) 5505 [arXiv:hep-ph/9808324].
47. Z. Fodor, S. D. Katz and A. Ringwald, *Phys. Rev. Lett.* **88** (2002) 171101 [arXiv:hep-ph/0105064].
48. Z. Fodor, S. D. Katz and A. Ringwald, *JHEP* **0206** (2002) 046 [arXiv:hep-ph/0203198].
49. K. Greisen, *Phys. Rev. Lett.* **16** (1966) 748.
50. G. T. Zatsepin and V. A. Kuzmin, *JETP Lett.* **4** (1966) 78 [*Pisma Zh. Eksp. Teor. Fiz.* **4** (1966) 114].
51. O. E. Kalashev, V. A. Kuzmin, D. V. Semikoz and G. Sigl, *Phys. Rev. D* **65** (2002) 103003 [arXiv:hep-ph/0112351].
52. D. S. Gorbunov, P. G. Tinyakov and S. V. Troitsky, *Astropart. Phys.* **18** (2003) 463 [arXiv:astro-ph/0206385].
53. D. V. Semikoz and G. Sigl, *JCAP* **0404** (2004) 003 [arXiv:hep-ph/0309328].
54. G. Gelmini, G. Varieschi and T. Weiler, arXiv:hep-ph/0404272.
55. Pierre Auger Observatory, <http://www.auger.org/>
56. IceCube, <http://icecube.wisc.edu/>
57. ANtarctic Impulse Transient Array, <http://www.ps.uci.edu/~anita/>
58. Extreme Universe Space Observatory, <http://www.euso-mission.org/>
59. Orbiting Wide-angle Light-collectors, <http://owl.gsfc.nasa.gov/>
60. Saltdome Shower Array, P. Gorham, D. Saltzberg, A. Odian, D. Williams, D. Besson, G. Frichter and S. Tantawi, *Nucl. Instrum. Meth. A* **490** (2002) 476 [arXiv:hep-ex/0108027].
61. T. Reiter, unpublished notes.
62. L. N. da Costa, W. Freudling, G. Wegner, R. Giovanelli, M. P. Haynes and J. J. Salzer, *Astrophys. J. Lett.* **468** (1996) L5 [arXiv:astro-ph/9606144].
63. A. Dekel *et al.*, *Astrophys. J.* **522** (1999) 1 [arXiv:astro-ph/9812197].
64. Akemo Giant Air Shower Array, <http://www-akemo.icrr.u-tokyo.ac.jp/AGASA/>
65. K. Abazajian, E. R. Switzer, S. Dodelson, K. Heitmann and S. Habib, arXiv:astro-ph/0411552.
66. G. J. Stephenson, T. Goldman and B. H. J. McKellar, *Int. J. Mod. Phys. A* **13** (1998) 2765 [arXiv:hep-ph/9603392].
67. A. Ringwald, T. J. Weiler and Y. Y. Y. Wong, in preparation.